Novel Poly(ethylene oxide) Grafted Polycarbazole Conjugated Freestanding Network Films via Anionic and Electrochemical Polymerization

Leiqiang Qin[1], Shimin Zhang[1], Jingkun Xu[1,3,*], Baoyang Lu[2,3,*], Xuemin Duan[2], Danhua Zhu[1], Yao Huang[1]

[1] Jiangxi Key Laboratory of Organic Chemistry, Jiangxi Science and Technology Normal University, Nanchang 330013, China
[2] School of Pharmacy, Jiangxi Science and Technology Normal University, Nanchang 330013, China
[3] School of Materials Science & Engineering, Shandong University, Jinan 250061, China
[*]E-mail: xujingkun@tsinghua.org.cn; lby1258@163.com.

Novel electroactive conjugated network of poly(ethylene oxide) grafted polycarbazole freestanding film poly[poly(N-epoxypropyl carbazole)] (PPEPC) was successfully achieved *via* anionic ring-open polymerization of N-epoxypropyl carbazole (EPC) and subsequently electrochemical polymerization of the resulting poly(N-epoxypropyl carbazole) (PEPC) in CH_2Cl_2-Bu_4NPF_6. Both doped and dedoped PPEPC films were partly soluble in strong polar solvents, such as dimethyl sulfoxide. In particular, remarkable enhancement of the fluorescence properties of dedoped PPEPC was observed in comparison with PEPC, and it was a good blue-light-emitter with maximum emission at 412 nm both in solution and solid state. Furthermore, the prepared PPEPC manifested favorable thermal stability and good mechanical properties, which can be easily bent or cut into variety of shapes. Scanning electron microscopy clearly showed that highly homogeneous PPEPC was formed on the electrode surface.

1. INTRODUCTION

Conducting polymers (CPs), as a novel generation of organic materials, have attracted considerable attention over the past decades [1]. In addition to the excellent electrical and optical

properties, the ease of preparation and modification of CPs have made them a popular choice for many applications, such as sensors, electrocatalysis, electrochromic displays, electroluminescent materials, solar cells, and polymer light-emitting diodes (PLED) [2-5]. Therefore, even to date, the pursuit of novel CPs films, especially with favorable mechanical properties as well as good optical properties, is still one of the main goals in the research and development of inherently CPs. However, the major aspect useful for many commercial applications is not the metal-like electrical property itself, but the combination of the electrical conductivity and the polymeric properties such as flexibility, low density, and ease of structural modification [6]. Recently, as a class of heteroaromatic organic compounds based on the dibenzopyrrole system, carbazole and its derivatives have been widely studied. Because of the intrinsic fluorescence and good hole-transporting ability, polycarbazole can act as photosensitizer and hole-transporting materials for optoelectronic devices [7-11] and memory devices [12] applications. The chemical or electrochemical synthesis of polycarbazole, belonging to a class of electrochemically active semiconducting polymers, has been used for applications such as photovoltaics, OLEDs, and FETs. Consequently, it is very necessary to prepare freestanding conducting polycarbazole film for their practical applications.

In recent years, the conversion of the "precursor polymers" to conjugated polymer network (CPN) films on conducting surfaces using electrochemical methods has been reported [13-16]. A variety of combinations should be possible for the design of a precursor polymer backbone and the "electroactive monomer" side group to form CPN films. The precursor is electropolymerized on the conducting substrate to form an insoluble CPN films which have both inter- and intra-molecular cross-linkages between the pendant monomer units. Generally, the properties of conjugated polymers are lies in the molecular structure, which can incorporate functional groups with specific electroactive properties to fine-tune structure-property relationships. For this reason, one of the thermoplastic materials with fairly high chemical, radiation, and hole-transporting ability as well as the effective electrically insulating properties, extensively studied in recent decades is poly(N-vinyl-carbazole) (PVK) [7,11,17]. However, in the previous studies, the low adhesion to different substrates and poor film-forming properties of PVK hinder its wide-scale employment in optoelectronic devices. It is known that the optoelectronic properties of PVK are determined primarily by the presence and relative disposition of carbazole group. Presumably, by passing from carbochain polymers to polyethers which contain analogous substituents with extensive systems of conjugated bonds, the photoelectric properties of the system would not change significantly. As a result of the appearance of ether linkages in the main chain, an improvement in the adhesion and film-forming properties should be quite expected among the carbazole-containing polyethers.

Based on this consideration, the electrochemical polymerization of poly(N-epoxypropyl carbazole) (PEPC) must be a better choice for the preparation of high quality polycarbazole films. On the other hand, as a cheapest and most promising type of photosemiconducting polymers, PEPC has been widely used in electrophotography for the manufacture of microfilms and colored slides [18-21]. However, PEPC was a non-conjugated ether polymer with pendant carbazole units. Many of its

applications were limited due to PEPC polymerized through the ether group was only in neutral forms. Owing to the polyether backbone and special pedant carbazole in PEPC, the secondary polymerization could be realized through the carbazole units, leading to the formation of a conjugated network polymer films with excellent fluorescence and mechanical properties.

In recent years, the electrodeposition of conducting polymers will obtain high quality free-standing polymer films [22-24] in some solvents. In this study, the secondary electrodeposition of high-quality frees-standing PPEPC film, was successfully achieved through the carbazole units from neutral solvents. The PEPC was chosen as the precursor polymer and its direct anodic oxidation led to the electrodeposition of freestanding and flexible PPEPC in $CH_2Cl_2-Bu_4NPF_6$ (0.1 mol L^{-1}), as shown in Scheme 1. The electrochemical, optical, electrical, mechanical properties, morphology, and thermal stability were investigated in detail.
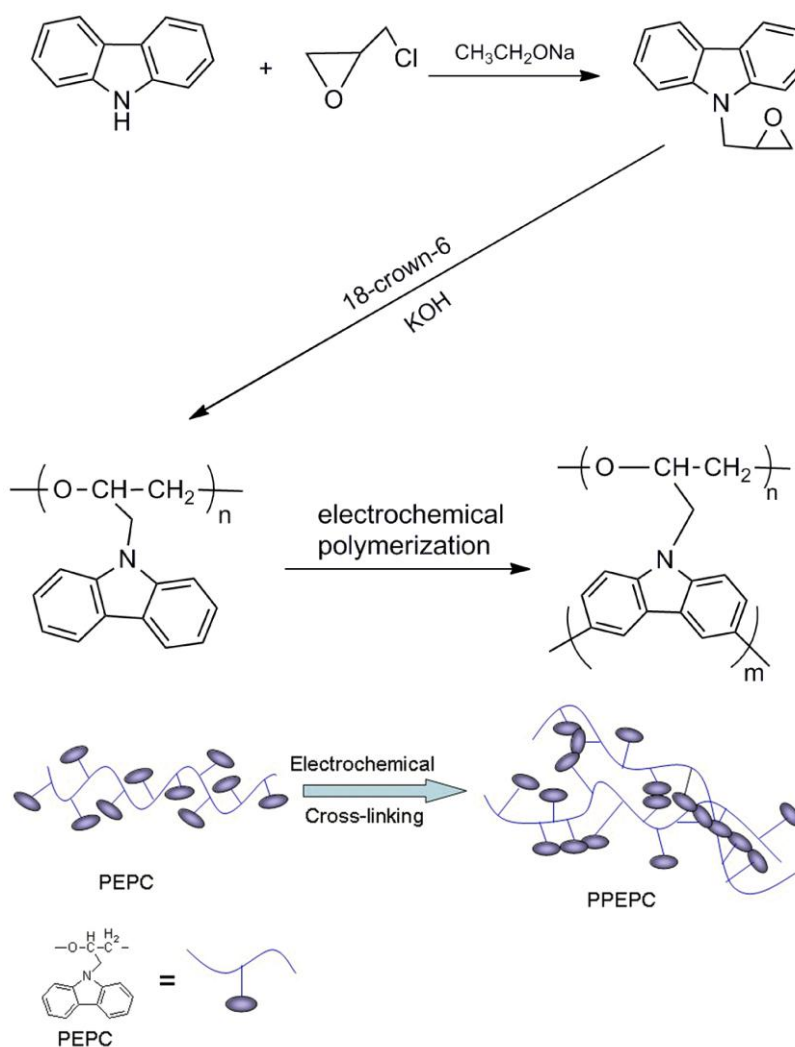
Scheme 1. Synthesis route and scheme for PEPC and PPEPC.

2. EXPERIMENTAL PART

2.1. Reagents

Carbazole (analytical grade; Acros Organics) was used after recrystallization and epichlorohydrin (99%; Aladdin) was used without further treatment. Dichloromethane and N, N-dimethylformamide (analytical grade) were products of Tianjin Bodi Chemicals Co. Ltd. and used after reflux distillation. Tetrabutylammonium hexafluorophosphate (Bu_4NPF_6, 98%; Acrocs Organics) was dried under vacuum at 60 ºC for 24 h before use. Dimethyl sulfoxide (DMSO, analytical grade; Tianjin Bodi Chem icals Co. Ltd.), and 25% ammonia (Ji'nan Chemical Reagent Company) were used as received without further purification. 18-crown-6 (99%; Aladdin), sodium methoxide, hydroxide, methanol, and toluene (Ji'nan Chemical Reagent Company) were used as received without further treatment.

2.2. Synthesis of N-epoxypropyl carbazole (EPC)

Carbazole (0.167 g, 1 mmol), sodium methoxide (0.16 g, 3 mmol) and 23 mL of anhydrous N, N-dimethylformamide were added to a three necked flask. The solution was heated to 40 ºC and dropwise added epichlorohydrin (1.28 g, 13 mmol), then stirred for 1 h and was allowed to cool to room temperature. After removal of the solvent, the remaining crude product was isolated by flash chromatography (silica gel, hexane/dichloromethane: 5/1) to isolate 1 as a white solid in 53% yield. ^{1}H NMR ($CDCl_3$, 400 MHz) δ (ppm) 8.11 (d, J = 7.6 Hz, 2H); 7.47 (d, J = 15.2 Hz, 4H); 7.24 (t, J = 15.6 Hz, 2H); 4.63 (d, J = 3.2 Hz, 1H); 4.41 (d, J = 16 Hz, 1H); 3.35 (d, J = 3.6 Hz, 1H); 2.81 (d, J = 4.0 Hz, 1H); 2.57 (t, J = 4.8 Hz, 1H).

2.3. Synthesis of Poly(N-epoxypropyl carbazole) (PEPC)

Potassium hydroxide (0.0176 g, 0.3 mmol), 18-crown-6 (0.1170 g, 0.4 mmol) and 8 mL methanol were added to a flask. When the solid dissolved, 8 mL toluene was added. The mixture was heated *in vacuo* until the volume of the distillate became half that of the volume of the original solution. Then a new portion of toluene was added and distilled again. This procedure was repeated five times. The solution was then cooled down to room temperature and filtered.

Polymerization of EPC was carried out in a flask equipped with nitrogen purge. 8 mL of the mentioned solution and EPC (0.8741 g) were added to the flask. The solution was heated at 90 ºC for 12 h. The resulting polymers were isolated by precipitation in hexane or in methanol and dried *in vacuo* at ambient temperature.

2.4. Electrochemical performance and synthesis

The electrochemical polymerization and examinations were performed in a one-compartment cell by the use of a potentiostat–galvanostat (Model 263A, EG&G Princeton Applied Research) under

computer control. The working and counter electrodes were Pt wires with diameter of 0.5 mm. They were placed 5 mm apart during the examinations. To obtain a sufficient amount of the polymer for characterization, Pt sheets and stainless steel (SS) sheets were employed as the working and counter electrodes, respectively. These electrodes were carefully polished with abrasive paper (1500 mesh), and cleaned successively with water and acetone, and then dried in air before each experiment. An Ag/AgCl electrode directly immersed in the solution served as the reference electrode and it revealed sufficient stability during the experiments. The polymer films grew potentiostatically, and their thickness was controlled by the total charge passed through the cell that was read directly from the current-time (I-t) curves by computer. After polymerization, the polymer films were washed repeatedly with anhydrous acetonitrile to remove the electrolyte, monomer, and oligomer. For spectral analyses, they were dedoped with 25% ammonia for 3 days and then washed repeatedly with pure water. Finally, they were dried at 60 ºC under vacuum for 24 h.

2.5. Apparatus

The electrical conductivity of the as-formed PPEPC films was determined by applying a conventional four-probe technique with the free-standing samples. Ultraviolet–visible (UV–*vis*) spectra were measured with a PerkinElmer Lambda 900 UV–*vis*–near–infrared (NIR) spectrophotometer. Infrared spectra were recorded using a Bruker Vertex 70 Fourier transform infrared (FT-IR) spectrometer with samples in KBr pellets. The fluorescence spectra were determined with an F-4500 fluorescence spectrophotometer (Hitachi). Gel permeation chromatography (GPC) measurements of the PEPC were performed in tetrahydrofuran with a Waters Breeze GPC system. Thermogravimetric analysis (TGA) was performed with a Pyris Diamond TG/DTA thermal analyzer (PerkinElmer). Scanning electron microscopy (SEM) measurements were made with a cold field emission scanning electron microscope ZEISS SIGMA.

3. RESULTS AND DISCUSSION

3.1. Electrochemical polymerization of PEPC

Various systems were chosen for the electrochemical polymerization of PEPC precursor. In THF containing Bu_4NPF_6, it is very difficult to obtain sufficient amount films. The main reason can be ascribed to the strong nucleophilicity of THF. It is well known that the electrochemical polymerization mechanism for the formation of the conducting polymer film is through the formation and coupling of radical cations [25]. THF, as a strong nucleophilic agent, can attack the intermediate radical cations during the polymerization. Therefore, the electropolymerization was interrupted by THF and PPEPC oligomers might be formed [17]. Therewith, we investigated the electrochemical polymerization of

PEPC in the traditional organic solvent acetonitrile, but the PEPC is partially dissolved in acetonitrile. Finally, dichloromethane containing 0.1 mol L^{-1} Bu_4NPF_6 in which PEPC with a good solubility and film-forming property was chosen as electrolyte. The onset oxidation potential was about 1.09 V (Fig. 1), which was lower than that of PVK (1.20 V) [26] in the same electrolyte.
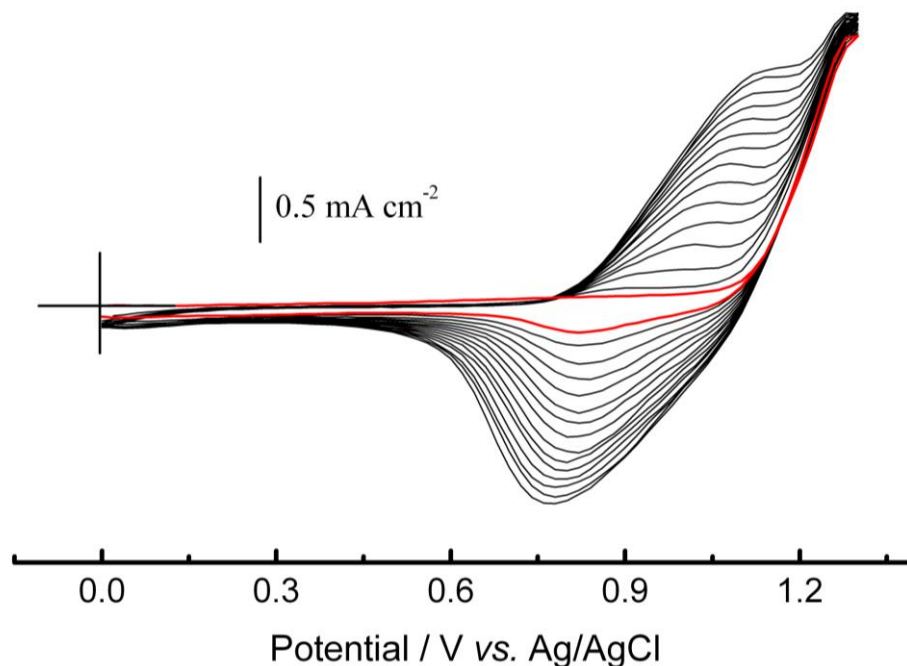

Figure 1. Cyclic voltammograms of PEPC (0.01 mol L^{-1}) in CH_2Cl_2 containing Bu_4NPF_6 (0.1 mol L^{-1}). Potential scan rate: 100 mV s^{-1}.

Cyclic voltammetry is a very useful method that qualitatively reveals the reversibility of electron transfer during the electropolymerization and also examines the electroactivity of the polymer films because the oxidation and reduction can be monitored in the form of a current potential diagram, that is, cyclic voltammogram (CV) [27]. The CVs of PEPC (Fig. 1) in $CH_2Cl_2-Bu_4NPF_6$ showed characteristic features of other conducting polymers during potentiodynamic syntheses [28-35] and high-quality metallic black films could be easily obtained. Successive potential scans led to the formation of a thin and uniform polymer film on the Pt electrode surface (green to black as the deposit thickened). The increase of anodic and cathodic peak current densities in CVs implied that the amount of the polymer film increased on the electrode surface. The broad redox waves of the polymer films may be ascribed to the wide distribution of the polymer chain length or the conversion of conductive species on the polymer main chain from the neutral state to polarons, from polarons to bipolarons, and finally from bipolarons to the metallic state [36]. The potential shift of the current wave maximum provided information about the increase of the electrical resistance of the polymer films and the overpotential needed to overcome this resistance. All these phenomena indicated that a high-quality and conducting PPEPC film was formed on the working electrode.

3.2. Electrochemistry of PPEPC films

In order to get a deeper insight into the electrochemical and environmental stability of as-formed polymer films and their electroactivity, the electrochemical behavior of PPEPC films was determined carefully by cyclic voltammetry in monomer-free electrolyte, as shown in Fig. 2. It can be clearly seen that steady-state CVs of the films represented broad anodic and cathodic peaks in the electrolyte. The potentials needed to oxidize or reduce the polymer films which prepared from the CH_2Cl_2 system were from 1.24 to 0.61 V in monomer-free $CH_2Cl_2-Bu_4NPF_6$. The peak current densities were proportional to potential scanning rates (inset of Fig. 2), indicating that the redox process is nondiffusional [37] and the electroactive polymer is well adhered to the working electrode surface.
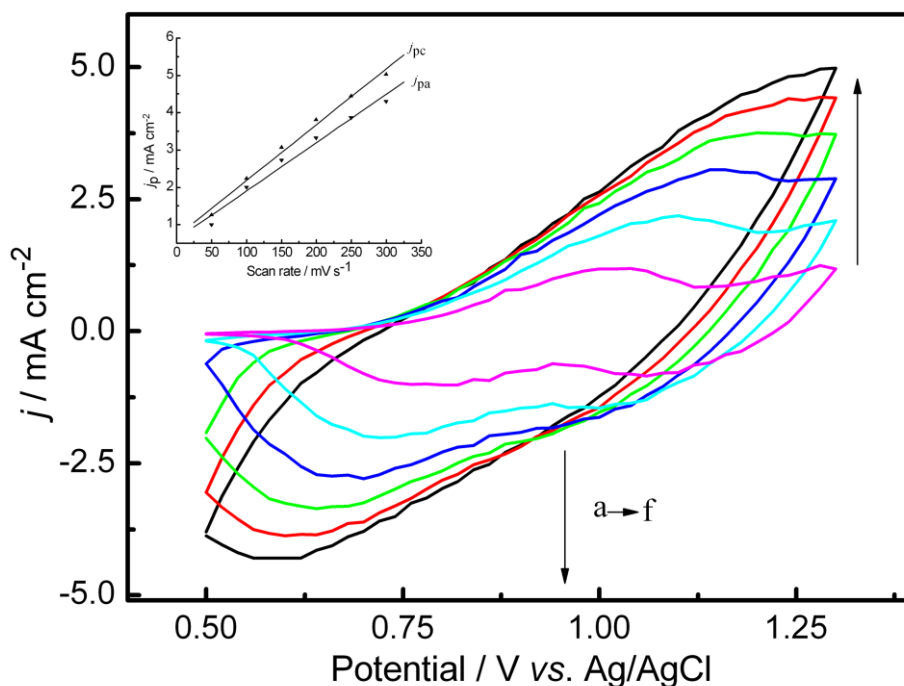

Figure 2. Cyclic voltammograms of PPEPC films electrochemically synthesized in CH_2Cl_2 containing Bu_4NPF_6 (0.1 mol L^{-1}) on the Pt electrode in monomer-free CH_2Cl_2 containing Bu_4NPF_6 (0.1 mol L^{-1}) at potential scan rates of 50 (a), 100 (b), 150 (c), 200 (d), 250 (e), and 300 mV s^{-1} (f). Inset: plots of redox peak current densities *vs.* potential scanrates. j_p is the peak current density, and $j_{p,a}$ and $j_{p,c}$ denote the anodic and cathodic peak current densities, respectively.

Furthermore, this film could be cycled repeatedly between the conducting (oxidized) and insulating (neutral) state without significant decomposition of the materials, indicating the high redox stability of the polymer.

3.3. FT-IR spectra

Vibrational spectra can provide much structural information for conducting polymers, especially for insoluble and infusible polymers. A comparison of the evolution of the vibrational modes appearing in conducting polymers and in some simpler related molecules acting as references usually facilitates the interpretation of the experimental absorption spectra. For the polymer using fused ring compounds as monomers, the vibrational spectra are particularly useful because they could be used to interpret the polymerization mechanism. Therefore, the FT-IR spectra of EPC (Fig. 3A), PEPC precursor (Fig. 3B) and dedoped PPEPC (Fig. 3C) obtained from CH_2Cl_2- Bu_4NPF_6 was examined. As can be seen from the figure, the peaks at 3062, 3016, and 2927 cm^{-1} in the spectrum of EPC can be assigned to the stretching of aroma, alkylene oxide or aliphatic C–H bonds. The bands in the region from 1640 to 1400 cm^{-1} were assigned to the stretching and shrinking modes of the aryl C–C, which were selectively broadened for PPEPC. The peak at 1324 cm^{-1} was the deformation vibration of C–N (Fig. 4A-C).
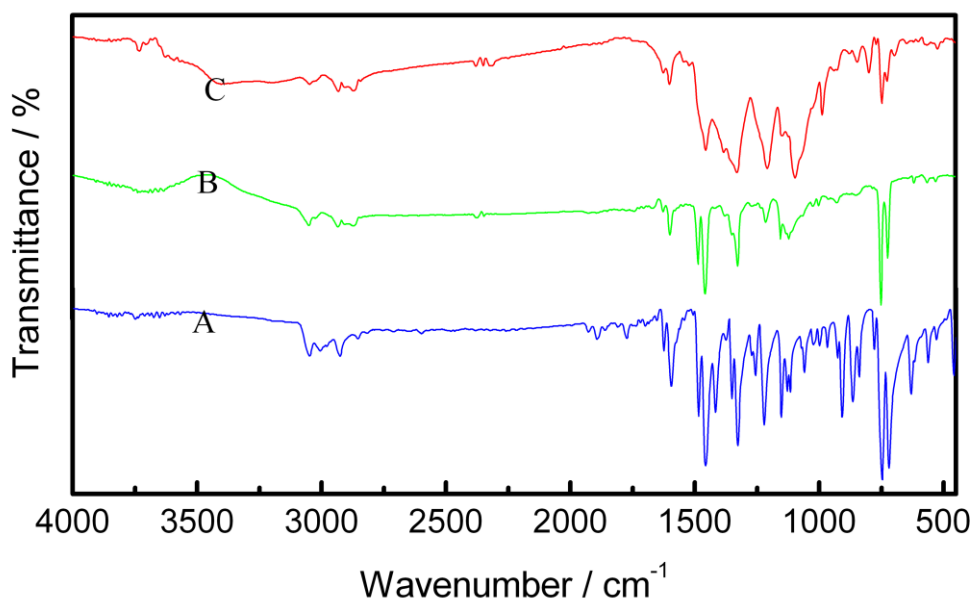

Figure 3. FT-IR spectra of EPC (A), PEPC (B), and dedoped PPEPC (C).

The medium strong peaks at 897, 860 and 832 cm^{-1} (Fig. 3A) were closely related to the stretching vibration of alkylene oxide, furthermore, the absence of the three bands (Fig. 3B, C) implies that the alkylene oxide changed into ether bond. In the spectrum of the EPC, the out-of-plane vibration of the four adjacent C–H bonds on ortho-disubstituted benzene appeared at 747 and 713 cm^{-1} [38]. The peaks located at 848 and 794 cm^{-1} (Fig. 3C) were ascribed to the out-of-plane deformation vibration of

1,2,4-trisubstituted benzene rings, which indicated the polymerization on the benzene ring. The peaks at 751 and 719 cm^{-1} implied that a small amount of independent carbazole units still existed in the polymer. Moreover, the augmented width and peak shifts of these bands from the PEPC to dedoped PPEPC manifested the occurrence of the electrochemical polymerization of PEPC. The broadening of the IR bands in the experimental spectra is due to that the resulting product composed of oligomers with wide chain dispersity. The vibrational peaks of the oligomers with different polymerization degrees have different IR shifts. These peaks overlap one another and produce broad bands with hyperstructures. Furthermore, there are some chemical defects on the polymer chains, which result from the inevitable overoxidation of the polymer. This also contributes to the band broadening of the experimental IR spectra. However, the peaks in the spectrum of PEPC were not obviously broadened compared with that of EPC, which is quite different from those of other polymers [29-35, 39]. This may be attributable to the relatively short chain length of the as-formed PEPC. It was in well accordance with the GPC measurement of the PEPC in tetrahydrofuran (it was demonstrated that the PEPC showed a number-average molar mass (M_n) of 2200 in tetrahydrofuran against polystyrene standards).
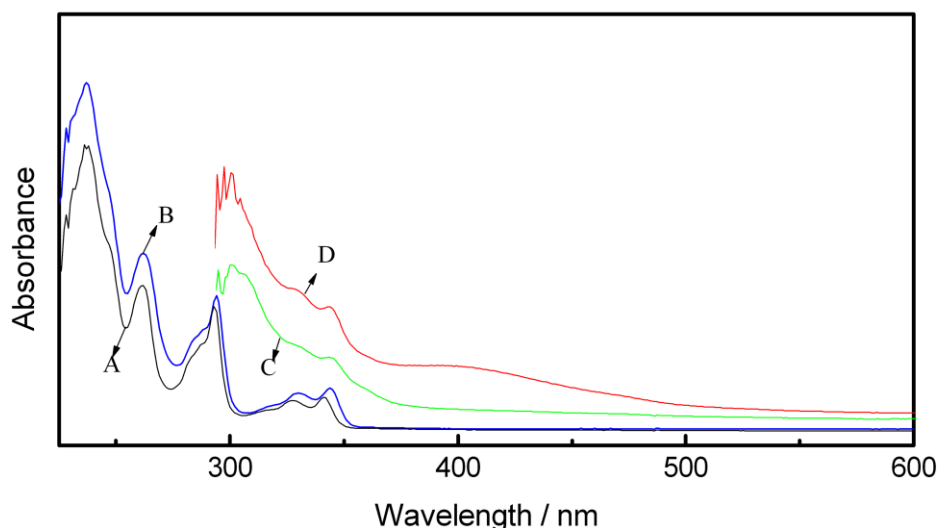
3.4. UV–vis absorption

Figure 4. UV-vis spectra of the EPC (A) and PEPC (B) in CH$_2$Cl$_2$; the dedoped PPEPC (C) and doped PPEPC (D) obtained from CH$_2$Cl$_2$ at a constant applied potential of 1.33 V *vs.* Ag/AgCl for 20 s on the ITO electrode.

The free-standing PPEPC films prepared from CH$_2$Cl$_2$–Bu$_4$NPF$_6$ were in the doped state and dark brown in color. The color of PPEPC films has been changed to brownish yellow, owing to the removal of the dopants, when they were dedoped by 25% ammonia. Doped and dedoped PPEPC films were partly soluble in strong polar solvents, such as DMSO, but almost insoluble completely in other common solvents. The UV–*vis* spectra of EPC, PEPC dissolved in CH$_2$Cl$_2$ and PPEPC deposited on

ITO transparent electrode were examined carefully, as shown in Fig. 4. The EPC showed several characteristic absorption peaks at 292, 326, and 340 nm (Fig. 4A), which were assigned to a single-electron π-π* transition of phenyl rings, containing two vibrational subbands. The spectrum of PEPC (Fig. 4B) was similar to EPC with characteristic absorption peaks at 294, 330, and 344 nm. The small red shift between the maximum absorptions of the EPC and the PEPC indicated that the polymer sequence of the ring-opening polymerization was not very long. UV−*vis* spectra of dedoped and doped PPEPC deposited on ITO transparent electrode were depicted in Fig. 4C and D. Both dedoped and doped PPEPC showed the same absorption at 300 and 344 nm. However, the doped polymer tailed off to more than 510 nm in comparison with those of EPC and PEPC (353 nm), which was mainly attributable to the increase in the conjugated chain length of the polymer [24, 33, 40].

3.5. Fluorescence spectra

Fluorescence spectra of the soluble part of dedoped PPEPC dissolved in DMSO and PPEPC deposited on ITO electrode were recorded, as shown in Fig. 5. For comparison, the spectrums of the EPC and PEPC were also included. It can be seen that the emission spectrum of the EPC emerged at 369 nm (Fig. 5A). The PEPC showed an emission peak at 371 nm (Fig. 5B), 3 nm red-shift than that of the EPC. This phenomenon was probably due to that the anionic ring-open polymerization product PEPC was non-conjugated, and the appearance of polyether backbone did not exhibit a great influence of fluorescence properties. The fluorescence spectrum of dedoped PPEPC dissolved in DMSO is also given in Fig. 5C. A dominant maximum at 412 nm can be clearly seen in the emission spectrum with a small shoulder at 366 nm. The bathochromic shift between the EPC and the dedoped PPEPC (about 43 nm) can be clearly seen from the figure.
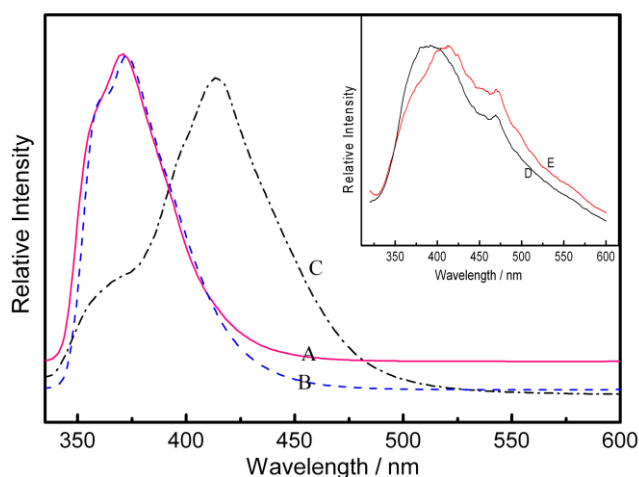

Figure 5. Emission spectra of EPC (A), PEPC (B) and dedoped PPEPC (C) electrochemically synthesized in CH₂Cl₂ solution. Solvent: DMSO. Inset: emission spectra of doped PPEPC (D) and dedoped PPEPC (E) prepared from CH₂Cl₂ at a constant applied potential of 1.3V *vs.* Ag/AgCl for 10 s on the ITO electrode.

It is mainly attributable to the elongation of the delocalized π-electron chain sequence resulting from the electropolymerization of pendant carbazole units. In solid state, the doped and dedoped PPEPC deposited on ITO transparent electrode showed two emission peaks at about 389 and 412 nm (Fig. 5D, E). It is different from previous research that the PPEPC showed hypsochromic shift compared with the emission of the polycarbazole and the dedoped PPEPC with the same emission peak at 412 nm in solution and solid state [33-35]. It is probably because the introduction of poly(ethylene oxide) backbone will decrease the polymers aggregation and reduce the number of polymerized carbazole in PPEPC due to increasing steric hindrance. All the above results show that PPEPC keep good blue light-emitting properties in solution and solid state, implying some potential applications in organic optoelectronics.

The fluorescence quantum yields ($\Phi_{overall}$) of the soluble samples were measured by using anthracene in acetonitrile (standard, $\Phi_{ref} = 0.27$) as the reference and calculated according to the well known method based on the expression:

$$\Phi_{overall} = (n^2 A_{ref} I / n^2_{ref} A I_{ref}) \times \Phi_{ref} \qquad (1)$$

Here, n, A, and I denote the refractive index of the solvent, the absorbance at the excitation wavelength, and the intensity of the emission spectrum, respectively. According to Eq. (1), the fluorescence quantum yield ($\Phi_{overall}$) of PEPC monomer was calculated to be only 0.034. The $\Phi_{overall}$ of the dedoped PPEPC was 0.092, distinctly improved compared with the monomer. Taking all these aspects together, as-formed PPEPC may be a very promising blue-light-candidate for optical displays used in optoelectronics, and is a very promising candidate for hole-transporting materials in LEDs.

3.6. Thermal properties of the polymers

Thermal degradation behavior of conducting polymers is very important for their potential applications. To investigate the thermal stability of PEPC and PPEPC films, thermogravimetric analytical experiments were performed under a nitrogen stream at a heating rate of 10 K min^{-1}, as shown in Fig. 6. From the figure, it can be clearly observed that there were both three-step weight losses for PPEPC (Fig. 6A) and PEPC (Fig. 6B). The polymer initially underwent a small weight decrease (about 17.11%) at relatively low temperature (from 290 K to 463 K), which may be attributed to the water evaporation and degradation of polyether chain or a few oligomers trapped in the polymer according to many authors [41]. With the gradual increasing of the temperature, a more prominent weight loss step (about 31.28%) was clearly found at 463 K < T < 907 K, such a prominent weight loss was closely related to the oxidizing decomposition of the skeletal PPEPC backbone chain structure. The following degradation after 907 K was probably caused by the overflow of the oligomers decomposed from PPEPC mentioned previously. In contrast, the PEPC was decomposing initially at 373 K and over at 540 K, shown that PPEPC has higher thermal stability than PEPC, which can be

mainly ascribed to the high thermal stability of benzene ring incorporation into the main chain of as-formed polymer films. In addition, even when the temperature reached 1100 K, the residual weight of PPEPC film was 45.85%, in contrast, the PEPC was 27.52%. Moreover, the value of PPEPC films is higher than the reported value of PPVK [17], and indicating the high thermal stability of PPEPC films. Therefore, from all these results, the conclusion can be easily drawn that the as-prepared PPEPC films display high decomposition temperatures, indicating that it can be applied in a wide temperature scale, which is of special significance for some potential applications.
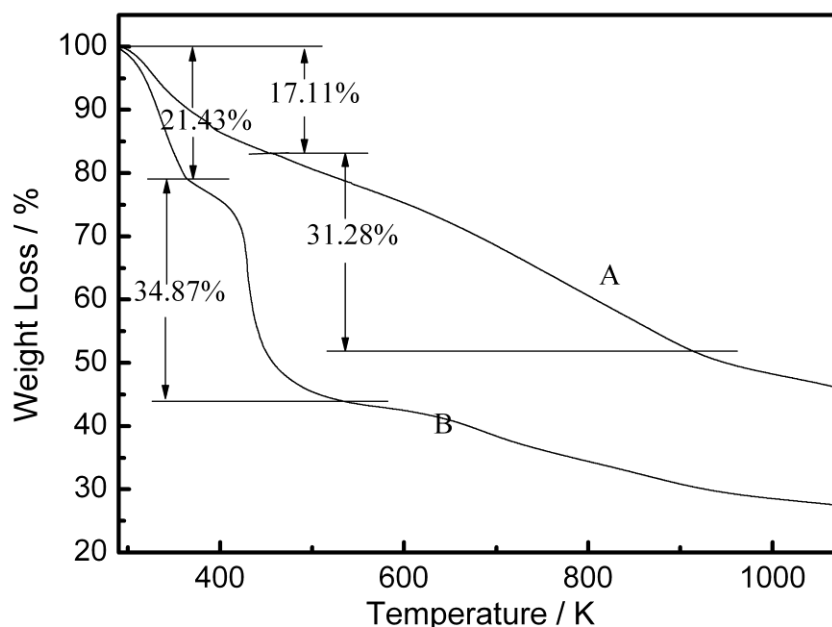

Figure 6. TGA curves of dedoped PPEPC (A) films obtained potentiostatically at 1.33 V *vs.* Ag/AgCl from CH_2Cl_2 and PEPC (B).

3.7. Conductivity and morphology

The electrical conductivity of the doped PPEPC, obtained from CH_2Cl_2 at a constant applied potential of 1.33 V *vs.* Ag/AgCl, was measured to be about 1.5×10^{-5} S cm^{-1}. The surface morphology of PPEPC film deposited on the ITO electrodes was investigated by scanning electron microscope (SEM), as shown in Fig. 7. Macroscopically, in both the doped and dedoped states, PPEPC film electrodeposited on the electrode surface was shiny, metal-like, homogeneous, compact and smooth. It can be peeled off from the electrode surface as a free-standing film, and the polymer film have good flexibility and can be cut like metal sheet with a knife or a pair of scissors into a variety of structures (Fig. 7A). Microscopically, the doped polymer films (Fig. 7B) displayed sphere-type growth processes form crowd globular surfaces [23,33,42]. The possible reason is that the amount of precursor is

sufficient to form a layer of thin film and then some microspheres (with diameters in the range from 300 nm to 1 μm). Nevertheless, the surface morphologies of the dedoped polymer films (Fig. 7C) transformed evidently, and the nanospheres were almost destroyed. These differences between the doped and dedoped polymer films were mainly due to the migration of counteranions out of the polymer films and their gradual solubility from the electrode to the solution during the dedoping processes [35,43], which broke the relatively smooth surfaces of doped polymer films.
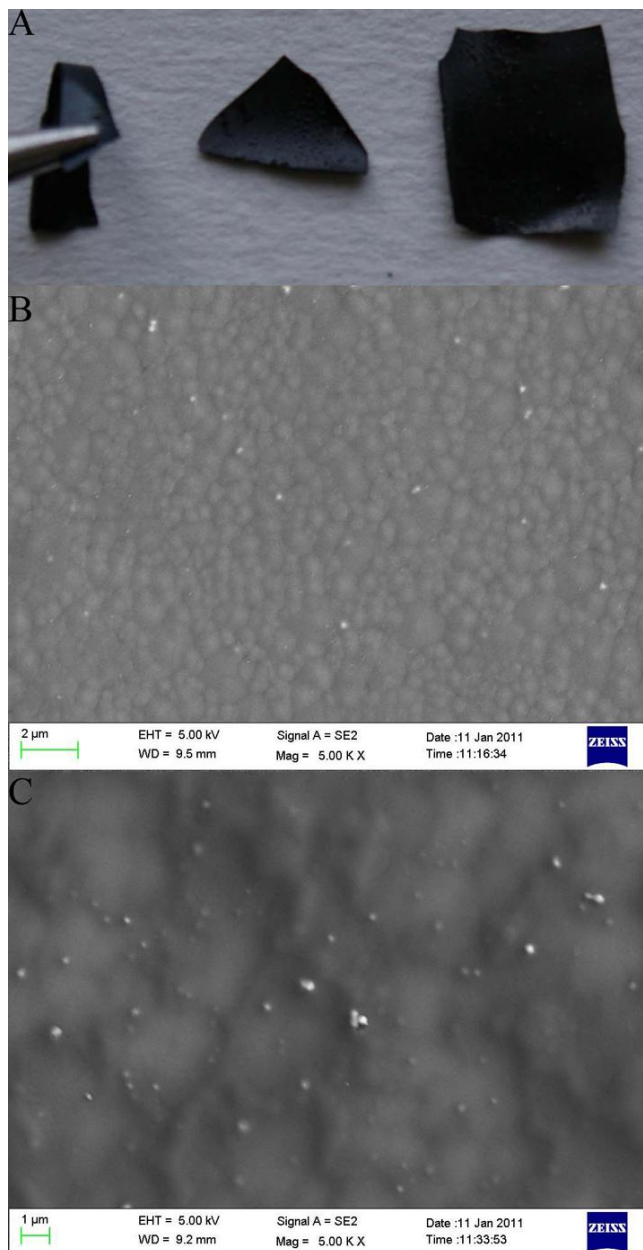

Figure 7. Photograph of free-standing conducting PPEPC films (A) prepared from CH_2Cl_2 containing Bu_4NPF_6 (0.1 mol L^{-1}) at a constant applied potential of 1.33 V *vs.* Ag/AgCl and SEM images of PPEPC films deposited electrochemically on ITO electrode for 20 s: doped PPEPC (B); dedoped PPEPC (C).

4. CONCLUSIONS

Detailed electrochemical cross-linking studies have been reported toward the CPN films formation for carbazole group pendanted poly[poly(N-epoxypropyl carbazole)] films. This work delineated the formation of CPN films using a precursor polymer where the carbazole moiety was dispersed by alkinyl ether from the polymer backbone. The direct anodic oxidation of the precursor polymer PEPC in CH_2Cl_2−TBAHFP led to facile electrodeposition of high-quality freestanding PPEPC films. The introduction of polyether backbone facilitated the formation of flexible, freestanding and well packed thin films. This enabled the efficient secondary polymerization of the carbazole side group to form a polymeric network. As-formed PPEPC films showed good redox activity and stability. Both UV-*vis* and FT-IR spectra of PPEPC films demonstrated that the polymerization probably occurred at the pendant carbazole units. Because of bring in the polyether chain, fluorescent spectral studies indicated that the PPEPC was a good blue-light emitter and the PPEPC maintained the same fluorescence properties in soluble and solid state. Furthermore, the resulting PPEPC manifested favorable thermal stability, smooth homogeneous surfaces and mechanical properties. With these attractive properties, PPEPC has many potential applications in various fields. Thus, it can be infer that the introduction of polyether backbone to other precursor polymer would significantly improve the film-forming properties and hold promise for the design of a new generation of optoelectronic materials.

References

1. T. A. Skotheim and J. R. Reynolds, *Handbook of Conducting Polymers*, 3rd ed CRC Press, Boca Raton, FL (2007).
2. R. Saraswathi, M. M. Verghese and B. D. Malhotra, *J. Appl. Polym. Sci.*, 74 (1999) 145.
3. S. Aravamuthan, C. L. Clement, S. Madhavan and K. S. V. Santhantham, *J. Power. Sources.*, 32 (1990) 1.
4. M. M. Verghese, M. K. Ram, H. Vardhan, B. D. Malhotra and S. M. Ashraf, *Polymer*, 38 (1996) 1625.
5. P. L. T. Boudreault, S. Wakim, N. Blouin, M. Simard, C. Tessier, Y. Tao and M. Leclerc, *J. Am. Chem. Soc.*, 129 (2007) 9125.
6. A. J. Heeger, *J. Phys. Chem. B.*, 105 (2001) 8475.
7. A. Baba, K. Onishi, W. Knoll and R. C. Advincula, *J. Phys. Chem. B.*, 108 (2004) 18949.
8. T. M. Fulghum, P. Taranekar and R. C. Advincula, *Macromolecules*, 41 (2008) 5681.
9. S. Lengvinaite, J. V. Grazulevicius, V. Jankauskas, S. Grigalevicius, *Synth. Met.*, 157 (2007) 529.

10. J. L. Li and A. C. Grimsdale, *Chem. Soc. Rev.*, 39 (2010) 2399.
11. M. S. Ho, C. Barrett, J. Paterson, M. Esteghamatian, A. Natansohn and P. Rochon, *Macromolecules*, 29 (1996) 4613.
12. C. Y. Huang, G. Q. Jiang and R. C. Advincula, *Macromolecules*, 41 (2008) 4661.
13. K. Lu, Y. L. Guo, Y. Q. Liu, C. A. Di, T. Li, Z. M. Wei, G. Yu, C. Y. Du and S. G. Ye, *Macromolecules*, 42 (2009) 3222.
14. K. J. Watson, P. S. Wolfe, S. T. Nguyen, J. Zhu and C. A. Mirkin, *Macromolecules*, 33 (2000) 4628.
15. P. Waenkaew, P. Taranekar, S. Phanichphant and R. C. Advincula, *Macromol. Rapid. Commun.*, 28 (2007) 1522.
16. A. Oral, S. Koyuncua and I. Kaya, *Synth. Met.*, 159 (2009) 1620.
17. J. K. Xu, W. Q. Zhou, H. P. Peng, S. Z. Pu, J. W. Wang and L. S. Yan, *Polym. J.*, 38 (2006) 369.
18. J. V. Grazulevicius, I. Soutar and L. Swanson, *Macromolecules*, 31 (1998) 4820.
19. T. X. Lav, F. Tran-Van, F. Vidal, S. Péralta, C. Chevrot, D. Teyssié, J. V. Grazulevicius, V. Getautis, H. Derbal and J. M. Nunzi, *Thin Solid Films*, 516 (2008) 7223.
20. K. M. Akhmedov, K. S. Karimov, I. M. Shcherbakova, Y. N. Porshnev and M. I. Cherkashin, *Russ. Chem. Rev.*, 59 (1990) 425.
21. R. Budreckiene, R. Lazauskaite, R. Kavaliunas and J. V. Grazulevicius, *Eur. Polym. J.*, 37 (2001) 983.
22. G. Q. Shi, S. Jin, G. Xue and C. Li, *Science*, 267 (1995) 994.
23. S. Jin and G. Xue, *Macromolecules*, 30 (1997) 5753.
24. B. Y. Lu, J. K. Xu, C. L. Fan, H. M. Miao and L. Shen, *J. Phys. Chem. B.*, 113 (2009) 37.
25. J. Roncali, *Chem. Rev.*, 92 (1992) 711.
26. S. Inaoka, D. B. Roitman and R. C. Advincula, *Chem. Mater.*, 17 (2005) 6781.
27. X. G. Li, M. R. Huang, W. Duan and Y. L. Yang, *Chem. Rev.*, 102 (2002) 2925.
28. H. T. Liu, Y. Z. Li, J. K. Xu, Z. G. Le, M. B. Luo, B. S. Wang, S. Z. Pu and L. Shen, *Eur. Polym. J.*, 44 (2008)171.
29. B. Y. Lu, L. Q. Zeng, J. K. Xu, Z. G. Le and H. Y. Rao. *Eur. Polym. J.*, 45 (2009) 2279.
30. G. Q. Shi, C. Li and Y. Q. Liang, *Adv. Mater.*, 11 (1999) 1145.
31. L. T. Qu and G. Q. Shi, *Chem. Commun.*, 24 (2004) 2800.
32. X. B. Wan, F. Yan, S. Jin, X. R. Liu and G. Xue, *Chem. Mater.*, 11 (1999) 2400.
33. J. K. Xu, H. T. Liu and S. Z. Pu, *Macromolecules*, 39 (2006) 5611.
34. B. Y. Lu, J. K. Xu, C. L. Fan, F. X. Jiang and H. M. Miao, *Electrochim. Acta.*, 54 (2008) 334.
35. B. Y. Lu, J. Yan, J. K. Xu, S. Y. Zhou and X. J. Hu, *Macromolecules*, 43 (2010) 4599.
36. M. Zhou and J. Heinze, *Electrochim. Acta.*, 44 (1999) 1733.
37. G. Sonmez, I. Schwendeman, P. Schottland, K. Zong and J. R. Reynolds, *Macromolecules*, 36 (2003) 639.
38. B. Meana-Esteban, C. Kvarnstrom and A. Ivaska, *J. Solid. State. Electrochem.*, 9 (2005) 450.
39. H. T. Liu, J. K. Xu, S. Z. Pu, M. B. Luo, Z. G. Le, *Mater. Lett.*, 61 (2007) 1392.
40. H. J. Bowley, D. L. Gerrard, W. F. Maddams, M. R. Paton, *Makromol. Chem.*, 186 (1985) 695.
41. J. C. Thieblemont, A. Brun, J. Marty, M. F. Planche and P. Calo, *Polymer*, 36 (1995) 1605.
42. M. L. Ma, H. T. Liu, J. K. Xu, Y. Z. Li, Y. Q. Wan, *J. Phys. Chem. C*, 111 (2007) 6889.
43. G. M. Nie, T. Cai, S. S. Zhang, Q. Bao, J. K. Xu, *Electrochim. Acta.*, 52 (2007) 7097.